


In Vitro Quantification of Gutter Formation and Chimney Graft Compression in Chimney EVAR Stent-Graft Configurations Using Electrocardiography-Gated Computed Tomography

Journal of Endovascular Therapy
 2018, Vol. 25(3) 387–394
 © The Author(s) 2018
 Reprints and permissions:
sagepub.com/journalsPermissions.nav
 DOI: 10.1177/1526602818762399
www.jevt.org


Simon P. Overeem, MSc^{1,2*} , Esmé J. Donselaar, MD^{3*}, Jorrit T. Boersen, PhD^{1,2,3}, Erik Groot Jebbink, PhD^{1,3}, Cornelis H. Slump, PhD¹, Jean-Paul P. M. de Vries, MD, PhD², and Michel M. P. J. Reijnen, MD, PhD³ 

Abstract

Purpose: To assess the dynamic behavior of chimney grafts during the cardiac cycle. **Methods:** Three chimney endovascular aneurysm repair (EVAR) stent-graft configurations (Endurant and Advanta VI2, Endurant and Viabahn, and Endurant and BeGraft) were placed in silicone aneurysm models and subjected to physiologic flow. Electrocardiography (ECG)-gated contrast-enhanced computed tomography was used to visualize geometric changes during the cardiac cycle. Endograft and chimney graft surface, gutter volume, chimney graft angulation over the center lumen line, and the D-ratio (the ratio between the lengths of the major and minor axes) were independently assessed by 2 observers at 10 time points in the cardiac cycle. **Results:** Both gutter volumes and chimney graft geometry changed significantly during the cardiac cycle in all 3 configurations ($p < 0.001$). Gutters and endoleaks were observed in all configurations. The largest gutter volume (232.8 mm³) and change in volume (20.7 mm³) between systole and diastole were observed in the Endurant-Advanta configuration. These values were 2.7- and 3.0-fold higher, respectively, compared to the Endurant-Viabahn configuration and 1.7- and 1.6-fold higher as observed in the Endurant-BeGraft configuration. The Endurant-Viabahn configuration had the highest D-ratio (right, 1.26–1.35; left, 1.33–1.48), while the Endurant-BeGraft configuration had the lowest (right, 1.11–1.17; left, 1.08–1.15). Assessment of the interobserver variability showed a high correlation (intraclass correlation > 0.935) between measurements. **Conclusion:** Gutter volumes and stent compression are dynamic phenomena that reshape during the cardiac cycle. Compelling differences were observed during the cardiac cycle in all configurations, with the self-expanding (Endurant-Viabahn) chimney EVAR configurations having smaller gutters and less variation in gutter volume during the cardiac cycle yet more stent compression without affecting the chimney graft surface.

Keywords

abdominal aortic aneurysm, aneurysm diameter, aneurysm model, cardiac cycle, chimney graft, endograft, dynamic computed tomography, ECG-gated computed tomography, endoleak, endovascular aneurysm repair, flow model, gutter, in vitro study, self-expanding stent-graft, stent compression, stent-graft, volume

Introduction

Endovascular aneurysm repair (EVAR) has become the standard treatment modality for abdominal aortic aneurysm (AAA). Around 30% of AAA patients are considered unsuitable for standard EVAR due to unfavorable proximal neck characteristics, such as short length or severe angulation. Juxtarenal AAAs account for ~15% of all AAAs.¹ Alternative treatment options include open repair, chimney EVAR

(CHEVAR), and fenestrated EVAR.^{2,3} CHEVAR combines a regular EVAR graft with chimney (or parallel) grafts (CGs) in the visceral arteries to maintain branch patency.^{4,5} A limitation of CHEVAR is the necessity for an upper extremity arterial access, which can lead to ischemic stroke in about 3% of the procedures.⁶ Furthermore, gutters may form due to a geometric mismatch between the endograft and CG and are associated with early type Ia endoleaks.^{7–9} In addition, compression of the CG, resulting from interaction

with the endograft and the aortic wall, may induce a risk of stent thrombosis.^{10,11}

Several studies have described the dynamics in EVAR geometry in the aorta during the cardiac cycle,^{12–14} but none of these studies assessed CHEVAR geometry and gutters in a dynamic setting. We hypothesized that a larger variation in gutter volume during the cardiac cycle might increase the risk of type Ia endoleak. Because of the changing volume during the cardiac cycle, the gutter may start functioning as a valve, by which the intra-aneurysmal pressure increases. Parodi et al¹⁵ showed that the mean pressure in the aneurysm sac increases in the presence of an endoleak, the extent of which is directly proportional to the endoleak size.

As described by several authors, computed tomography angiography (CTA) imaging of low-flow endoleaks leads to significantly different enhancement peaks compared with the lumen of the abdominal aorta.^{16,17} The dynamic behavior of gutter volume in combination with imprecise acquisition timing might lead to an underestimated or undiagnosed gutter-related endoleak. Our previous research suggested that progression of the native aneurysm sac diameter without clear type Ia endoleak might be the result of suboptimal imaging.⁹ Although there is no best CTA scan protocol to identify low-flow gutters as well as all endoleak types, follow-up imaging of CHEVAR patients should consist of multiphase contrast-enhanced CT or electrocardiography (ECG)-gated contrast-enhanced CT. The latter imaging protocol was used in this study to quantify the dynamic geometric behavior of 3 CHEVAR configurations during the cardiac cycle.

Methods

In Vitro Models

In vitro models (Figure 1) were manufactured by Elastrat Inc (Geneva, Switzerland), using geometry based on the average measurements from the preoperative CT scans of 25 AAA patients. Three different CHEVAR configurations were implanted by an experienced vascular surgeon (M.R.). All used the Endurant endograft (ETBF3216C166EE, ETLW1616C124EE; Medtronic Inc, Minneapolis, MN, USA), which was chosen because of its widespread use in CHEVAR⁸ with either self-expanding or balloon-expandable stents and its recent approval for use with the chimney graft technique based on the PROTAGORAS study (n=128).¹¹ The

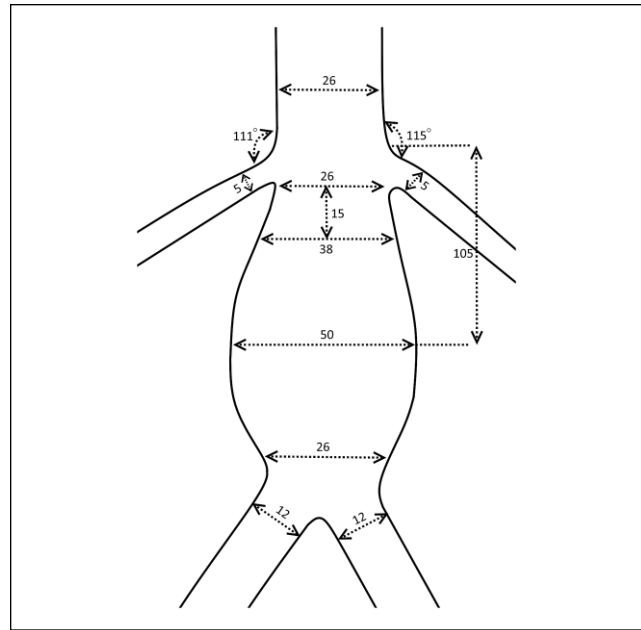


Figure 1. Geometry of the silicone model used for the 3 different chimney endovascular aneurysm repair configurations. Dimensions are in millimeters or degrees (°).

CGs included a 6×52-mm self-expanding Viabahn stent-graft (W.L. Gore & Associates Inc., Flagstaff, AZ, USA) and 2 types of balloon-expandable covered stents: a 6×58-mm Advanta V12 (Atrium Maquet Getinge Group, Mijdrecht, the Netherlands) and a 6×52-mm BeGraft (Bentley Innomed GmbH, Hechingen, Germany).

The top of the aortic endograft (24% oversized according the Medtronic CHEVAR instructions for use) was positioned flush below the level of the distal edge of the superior mesenteric artery (SMA). The right CG was positioned parallel to the endograft in all configurations, with the top at the level of the lower edge of the SMA. The left CG was positioned with its proximal end at the midline of the SMA orifice. The Endurant was deployed first, followed by positioning and deployment of the CGs. In all models, the Endurant was postdilated with a compliant balloon (Reliant; Medtronic) to adapt to the model, while a 6-mm angioplasty balloon was inflated simultaneously in the CGs to prevent stent compression. The configurations [Endurant-Advanta (EA), Endurant-Viabahn (EV), and Endurant-BeGraft (EB)] were flushed with water at 37°C to allow maximal

¹MIRA Institute for Biomedical Technology and Technical Medicine, University of Twente, Enschede, the Netherlands

²Department of Vascular Surgery, St Antonius Hospital, Nieuwegein, Utrecht, the Netherlands

³Department of Vascular Surgery, Rijnstate Hospital, Arnhem, the Netherlands

*Simon P. Overeem and Esmé J. Donselaar contributed equally to this work and have shared first authorship.

Corresponding Author:

Simon P. Overeem, Department of Vascular Surgery, St Antonius Hospital, Koekoekslaan 1, Nieuwegein, Utrecht 3435CM, the Netherlands.
Email: s.overeem@antoniusziekenhuis.nl

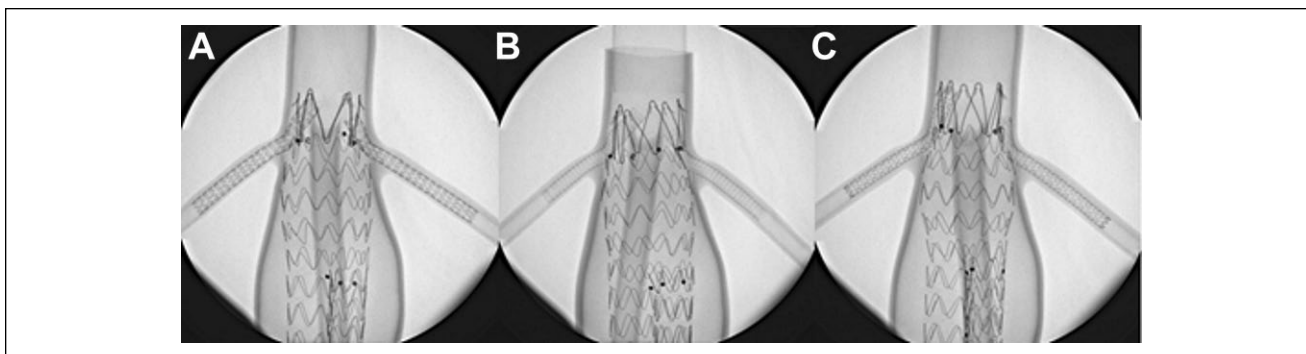


Figure 2. Anteroposterior angiograms of the 3 in vitro chimney endovascular aneurysm repair configurations: (A) Endurant-Advanta, (B) Endurant-Viabahn, and (C) Endurant-BeGraft.

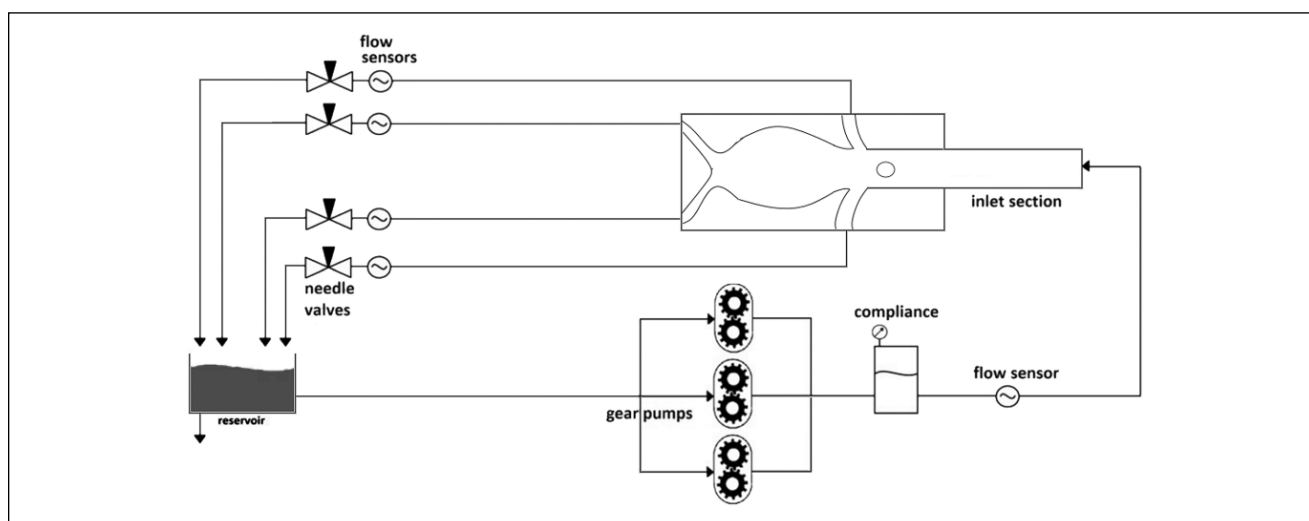


Figure 3. Schematic overview of the flow setup.

expansion of the nitinol stents. Angiographic images of the configurations are displayed in Figure 2.

Flow Model

A flow model generating physiologic flow at resting condition as previously described¹⁸ was used with the following settings: 60 beats/minute, diastolic pressure of 90 mm Hg, systolic pressure of 120 mm Hg, and mean flow 1.6 L/min (range 0.0–5.0 L/min). The 4 outflow vessels, 2 iliac and 2 renal arteries, all accounted for a quarter of the total flow. The flow rate was continuously assessed at 60 Hz with 5 flow sensors [Cynergy3, type UF8B (Cynergy3 Components Ltd, Dorset, UK) and FCH-m-POM-LC (BIOTECH e.K., Vilshofen, Germany)]. A blood mimicking fluid based on water, glycerol, and sodium iodide (47.4%, 36.9%, 15.7%, respectively) with a viscosity of 4.3 cP was used.¹⁹ Placing the models in a container with a water level 5.0 cm above the model accounted for the intra-abdominal pressure (5–7 mm

Hg). Compliance directly below the renal arteries was comparable to a healthy aorta.^{20,21} Each configuration was placed in the flow model for 5 minutes before starting the CTA. A schematic representation of the setup is shown in Figure 3.

EKG-Gated CT Scan

Images were acquired with a 256-slice CT scanner (Brilliance iCT; Philips Healthcare, Eindhoven, the Netherlands). Scanning parameters were similar to conventional CTA in a clinical setting and included a 120-kV tube voltage, 242-mA tube current (399 mA·s), 125×0.625-mm collimation, 10 unidirectional 1.65-second scan phases, 1.0-mm slice thickness, and a 200-mm field of view on the long axis. A matrix size of 512×512 pixels was used with a pixel spacing of 0.684 mm. A contrast bolus (Xenetix 350; Guerbet, Paris, France) tracking threshold of 150 HU was used to initiate the scan and to increase the differences in intensities between the lumen, endograft, CGs, and vessel wall.

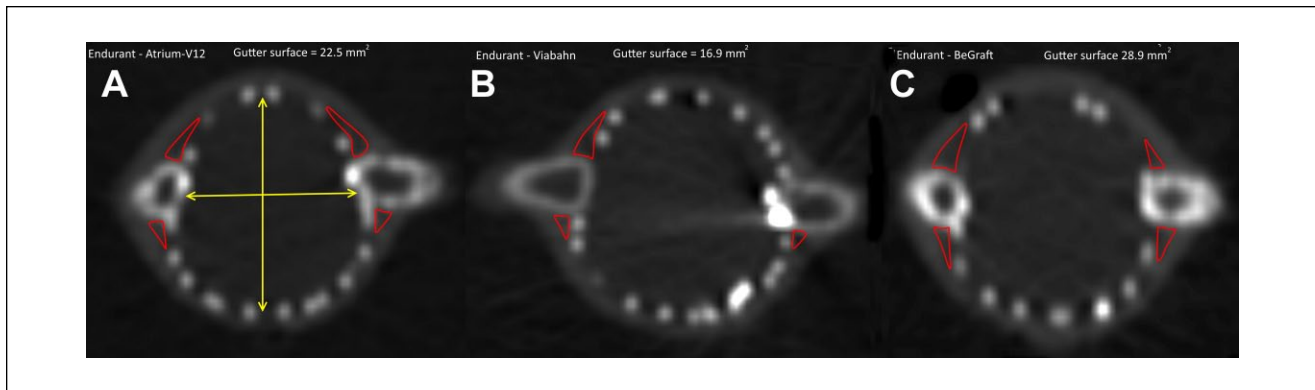


Figure 4. Computed tomography (CT) slices at the midline of the right renal artery perpendicular to the central lumen line for measurement of the gutter surfaces in the (A) Endurant-Advanta, (B) Endurant-Viabahn, and (C) Endurant-BeGraft configurations.

Measurements

Endograft, CG, and gutter surfaces were measured independently by 2 observers (S.O. and E.D.) using 3Mensio Vascular software (Pie Medical, Bilthoven, the Netherlands). Each model was analyzed once per observer, so in total 3 dynamic CT scans were evaluated. All surface calculations were performed over a central lumen line (CLL) perpendicular to the flow lumen on subsequent 1-mm slices using the polygon region of interest tool. Measurements were conducted in all 10 phases per series to assess the geometric changes during the cardiac cycle. An example of measured gutter surfaces is shown in Figure 4. Gutter types were characterized according to the scheme developed by Overeem et al⁹ (Figure 5), in which type A gutters originate at the proximal fabric of an endograft, type B gutters refer to loss of apposition of the CG in the branch vessel, and type C gutters start below the fabric of the endograft.

Measurements of endograft and gutter surfaces started at the beginning of the endograft fabric, 1 to 2 mm above the markers, and ended at the level where the endograft lost wall apposition. The CG surface started at the beginning of the CG fabric and ended 2.0 mm in the renal artery, where the surface remained constant. The average surface of the CGs and endograft over the CLL at all 10 time points was used for analysis. The surface measurements were performed to identify the dynamic behavior of the geometry of the configurations. Large changes in CG surface indicated high compliance of the stent.

The ratio of the length of the major and minor axes of the surface area, the D-ratio, was used to determine both endograft and CG compression, with a D-ratio of 1 equaling a circle. A D-ratio >1 described a more oval shape, and thus CG compression. The absolute difference and relative increase between the largest and smallest surfaces, volumes, and D-ratio during the cardiac cycle were determined.

Statistical Analysis

Interobserver variability was assessed between observers using the intraclass correlation coefficient (ICC). An ICC >0.8 is considered to indicate a low variability between observers. A Student *t* test was used to test significance between the measurements performed per configuration during the cardiac cycle. The threshold of statistical significance was $p < 0.05$. Statistical analysis was performed with SPSS software (version 22; IBM Corporation, Armonk, NY, USA).

Results

The geometric changes in gutter volume, endograft surface, chimney volume, and the D-ratio during the cardiac cycle are shown in Table 1. Four gutters were observed in each of the configurations (Table 2), although the types differed.⁹ In all configurations a gutter-related type Ia endoleak was observed, since contrast was seen in the aneurysm sac directly after bolus administration.

Gutter volumes and changes in gutter volume during the cardiac cycle differed significantly in all 3 configurations ($p < 0.001$). The largest gutter volume (232.8 mm^3) and change in volume (20.7 mm^3) between systole and diastole was observed in the EA configuration. These values, respectively, were 2.7- and 3.0-fold higher compared with the EV configuration and 1.7- and 1.6-fold higher compared with the EB configuration.

The differences in D-ratio of the Endurant endograft during the cardiac cycle were small in all configurations (EA, 1.13–1.18; EV, 1.13–1.15; and EB, 1.21–1.24). In addition, change in D-ratio between systole and diastole was comparable for all 3 configurations (EA, 0.05; EV, 0.03; and EB, 0.03).

The D-ratios for both the left and right chimneys were the lowest for the EB configuration (right, 1.11–1.17; left, 1.08–1.15) and the highest for the EV configuration (right,

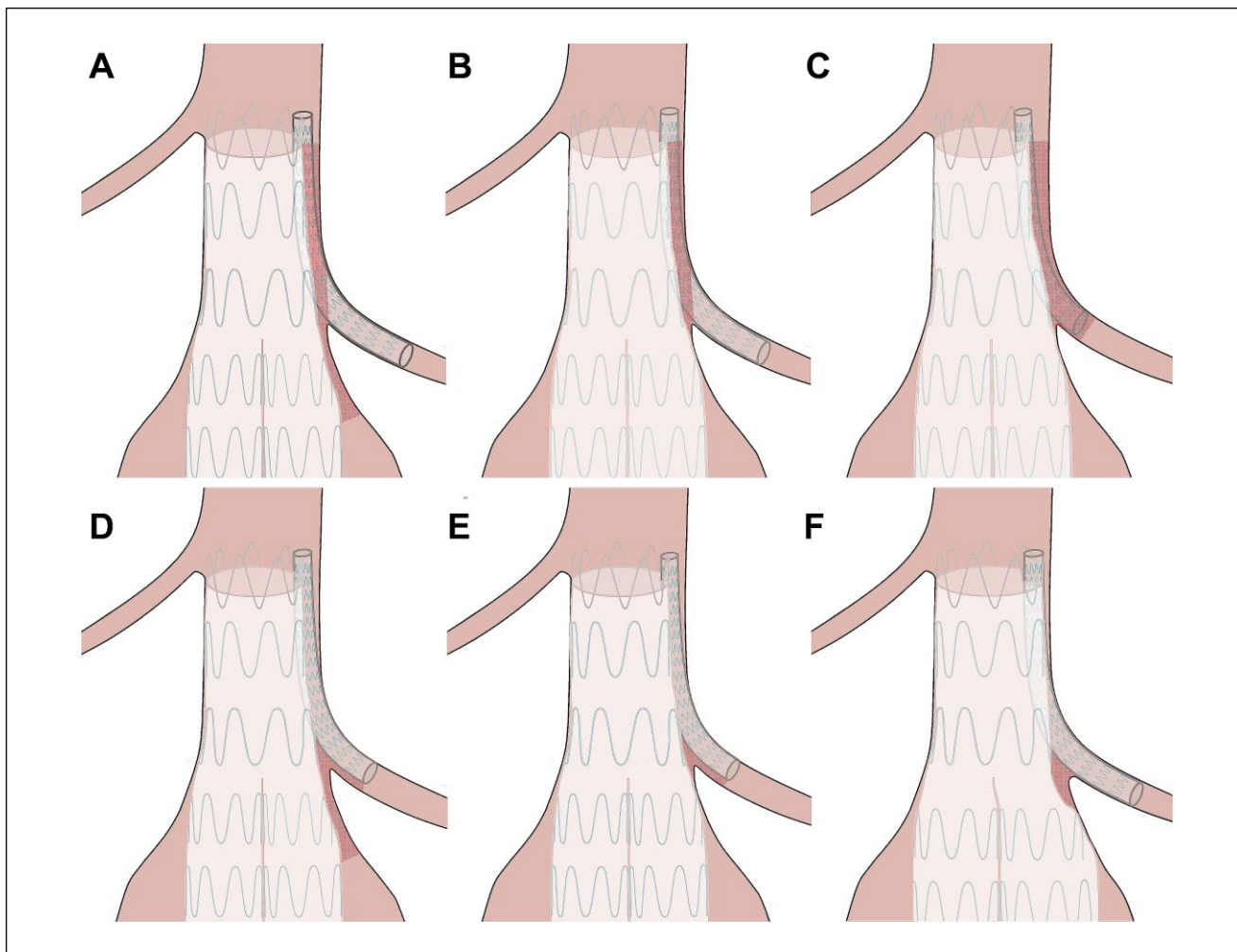


Figure 5. Overview of the gutter types according to the classification of Overeem et al⁹: (A) type A1, (B) type A2, (C) type A3, (D) type B1, (E) type B2, and (F) type C.

1.26–1.35; left, 1.33–1.48). The average chimney surface measurements (left, 26.6–30.7 mm²; right, 26.9–29.2 mm²), as well as the change in surface during the cardiac cycle (left 4.1, mm²; right 2.3 mm²), were also the highest in the EV configuration. The average surface and change in surface in the EB configuration during the cardiac cycle were almost similar for the right (18.4–19.2 mm² and 0.8 mm², respectively) and left (19.8–21.6 mm² and 0.8 mm², respectively) chimneys. There was a statistically significant difference in D-ratio and average surface during the cardiac cycle in all 3 configurations ($p < 0.001$).

The angulation of the right chimney (EA, 19.5°; EV, 13.2°; EB, 24.3°) differed from the left CG (EA, 38.3°; EV, 23.1°; EB, 57.3°) in all configurations, with the EB configuration having the largest angulation. Interestingly, the angulation of the CGs per configuration did not change significantly during the cardiac cycle. A high correlation was

found for all measurements (Table 3), being the lowest in the left chimney surface measurements with an ICC of 0.935.

Discussion

The importance of CG type in CHEVAR is well recognized in clinical practice.^{11,22,23} In the current study, differences were found in endograft surface, CG compression, and gutter volume in the different configurations during the cardiac cycle. In all 3 configurations, type Ia endoleaks were observed in conjunction with type A1 gutters (high risk). Video 1 details the contrast enhancement patterns during the cardiac cycle (Figure 6). Interestingly, enhancement of a gutter leak was present only in systole, which highlights the importance of CTA timing when using static CTA images in clinical follow-up. Although the majority of primary type Ia

Table 1. Geometric Changes in Gutter Volume, Endograft Surface, and the Chimney Grafts During the Cardiac Cycle.

	Endurant/Advanta V12	Endurant/Viabahn	Endurant/BeGraft
Gutter volume, mm ³			
Minimum	212.1	79.9	126.0
Maximum	232.8	86.7	138.8
Difference	20.7	6.8	12.8
Endograft surface, mm ²			
Minimum	671.7	734.8	652.2
Maximum	693.7	746.1	676.2
Difference	22.0	11.3	24.0
D-ratio of endograft			
Minimum	1.13	1.13	1.21
Maximum	1.18	1.15	1.24
Difference	0.05	0.02	0.03
Chimney surface right			
Minimum, mm ²	22.8	26.9	18.4
Maximum, mm ²	24.8	29.2	19.2
Difference, mm ²	2.0	2.3	0.8
Angulation, deg	19.5	13.2	24.3
D-ratio right			
Minimum	1.16	1.26	1.11
Maximum	1.25	1.35	1.17
Difference	0.09	0.09	0.06
Chimney surface left			
Minimum, mm ²	19.8	26.6	22.9
Maximum, mm ²	21.6	30.7	23.9
Difference, mm ²	0.8	4.1	1.0
Angulation, deg	38.3	23.1	57.3
D-ratio left			
Minimum	1.30	1.33	1.08
Maximum	1.36	1.48	1.15
Difference	0.06	0.15	0.07

Table 2. Number of Gutter Types per Stent Configuration.

Gutter Types ^a	Endurant/Advanta V12	Endurant/Viabahn	Endurant/BeGraft
A			
A1	2	1	1
A2	0	0	0
A3	1	2	2
B			
B1	0	0	0
B2	0	0	0
C			
C	1	1	1

^aType A gutters originate at the proximal fabric of an endograft, type B gutters result from loss of apposition of the chimney stent-graft in the branch vessel, and type C gutters start below the fabric of the endograft. Subtype A1 continues in the aneurysm sac, A2 extends into the visceral artery, and A3 terminates above the aneurysm sac or branch vessel. Subtype B1 gutter connects with the aneurysm sac, and B2 gutters have no connection with the aneurysm sac. Subtype C gutter describes an enclosed volume, originating below the proximal start of the endograft fabric and without connection to the aneurysm sac or proximal or distal chimney end.

gutter endoleaks resolve spontaneously over time (88% in a study by Ullery et al²⁴), treatment may also be required, particularly in larger endoleaks.²⁵⁻²⁷

The EA configuration had the largest gutter volume and a substantial change in gutter volume, which might increase the risk of type Ia endoleak. In contrast, the EV configuration

Table 3. Variability Between Observers.

	Intraclass Correlation Coefficient
Endograft surface (n=282)	0.988 (95% CI 0.985 to 0.991)
Chimney (left) surfaces (n=479)	0.935 (95% CI 0.922 to 0.945)
Chimney (right) surfaces (n=598)	0.963 (95% CI 0.957 to 0.969)
Gutter volume (n=120)	0.957 (95% CI 0.939 to 0.970)

Abbreviation: CI, confidence interval.

had the lowest gutter volume and only a small change in gutter volume during the cardiac cycle. However, the CG D-ratio and the change in CG D-ratio were the largest in the EV configuration. This is likely related to the relatively low radial force of the Viabahn in relation to the Endurant, causing stent compression. The D-ratio seems a logical way of expressing stent compression; however, most studies report stent compression as a percentage of the original lumen.¹⁴ Mestres et al²⁸ performed an interesting in vitro study describing different endograft/parallel stent combinations, concluding that the combination of self-expanding stents (Viabahn) and Endurant endografts should be avoided because of the risk of stent compression. Nevertheless, in the current study, the average endograft surface was found to be the largest in the EV configuration, indicating that compression does not immediately imply a stenosis.

The 2 balloon-expandable CGs in the study had different characteristics. While gutter volumes and changes in gutter volume during the cardiac cycle were lower in the BeGraft CG, the D-ratios were also lower. This observation may seem counterintuitive as there seems to be an inverse relation between the D-ratio and gutter volume. This result, however, could be explained by the difference in stent designs. The Advanta V12 consists of 316L steel that is encapsulated with polytetrafluoroethylene (PTFE), rendering the stent stiffer compared to the BeGraft, which is a cobalt chromium stent with a single PTFE layer. Reduced flexibility could cause kinking and, as such, a high D-ratio. This hypothesis is confirmed by the observation that the angulation was larger in the BeGraft, indicating a more parallel position of the CG. Nevertheless, Tessarek et al²⁹ have shown comparable radial compression force values of both stents (0.21 vs 0.24 N/mm to achieve 50% diameter reduction).

The average maximum surfaces of the left and right CGs differed significantly, more than the change in chimney surface during the cardiac cycle, presumably caused by a combination of CG positioning and the geometry of the model. This highlights the importance of CG positioning, which

might have a larger impact on conformability and gutter volume than chimney type and requires further research.

Limitations

First, the models do not replicate the elasticity of the native aorta, which might result in different stent-graft conformation and behavior. Second, the models were tested under ideal resting conditions, without a complex neck anatomy and/or calcifications. Only 1 model per configuration was tested.

Another limitation of the study is the position of the CGs. As shown in Figure 2, the proximal edge of the stent-graft was positioned at the level of the renal arteries. With the current knowledge of proper CHEVAR technique, the main body would have been positioned higher and the CGs would have been positioned more parallel to extend the seal in the suprarenal aortic neck.

Third, although the distinct CG designs and materials are the essence of this study, these individual materials have particular morphologic appearances on CT images. The greater or lesser extent of scattering of the metal struts influenced the estimated CG surface during measurement. Therefore, the measured surface may be slightly overestimated compared to the true CG surface.

Conclusion

Gutters are a dynamic phenomenon, with a volume that changes throughout the cardiac cycle. The configuration with a self-expanding chimney stent-graft had the lowest gutter volume and smallest change in gutter volume during the cardiac cycle. However, this resulted in the highest CG compression without affecting the CG surface. Compelling differences were also observed in the two studied balloon-expandable CGs. Further research with more endograft-CG configurations, different positioning of the CGs, and varying endograft oversizing should establish the best CHEVAR configuration in clinical practice.

Declaration of Conflicting Interests

The author(s) declared the following potential conflicts of interest with respect to the research, authorship, and/or publication of this article: Jean-Paul P. M. de Vries is a consultant for Medtronic.


Funding

The author(s) received no financial support for the research, authorship, and/or publication of this article.

Supplemental Material

The online video is available at <http://journals.sagepub.com/doi/suppl/10.1177/1526602818762399>

ORCID iDs

Simon P. Overeem  <https://orcid.org/0000-0002-3282-6654>

Michel M. P. J. Reijnen  <https://orcid.org/0000-0001-7641-1322>

References

- Jongkind V, Yeung KK, Akkersdijk GJM, et al. Juxtarenal aortic aneurysm repair. *J Vasc Surg.* 2010;52:760–767.
- Bastos Gonçalves F, Hoeks SE, Teijink JA, et al. Risk factors for proximal neck complications after endovascular aneurysm repair using the Endurant stentgraft. *Eur J Vasc Endovasc Surg.* 2015;49:156–162.
- Zarins CK, Bloch DA, Crabtree T, et al. Stent graft migration after endovascular aneurysm repair: importance of proximal fixation. *J Vasc Surg.* 2003;38:1264–1272.
- Suominen V, Pimenoff G, Salenius J. Fenestrated and chimney endografts for juxtarenal aneurysms: early and midterm results. *Scand J Surg.* 2013;102:182–188.
- Resch TA, Sonesson B, Dias N, et al. Chimney grafts: is there a need and will they work? *Perspect Vasc Surg Endovasc Ther.* 2011;23:149–153.
- Katsargyris A, Oikonomou K, Klonaris C, et al. Comparison of outcomes with open, fenestrated, and chimney graft repair of juxtarenal aneurysms: are we ready for a paradigm shift? *J Endovasc Ther.* 2013;20:159–169.
- Moulakakis KG, Mylonas SN, Dalainas I, et al. The chimney-graft technique for preserving supra-aortic branches: a review. *Ann Cardiothorac Surg.* 2013;2:339–346.
- Li Y, Zhang T, Guo W, et al. Endovascular chimney technique for juxtarenal abdominal aortic aneurysm: a systematic review using pooled analysis and meta-analysis. *Ann Vasc Surg.* 2015;29:1141–1150.
- Overeem SP, Boersen JT, Schuurmann RCL, et al. Classification of gutter type in parallel stenting during endovascular aortic aneurysm repair. *J Vasc Surg.* 2017;66:594–599.
- Scali ST, Feezor RJ, Chang CK, et al. Critical analysis of results after chimney endovascular aortic aneurysm repair raises cause for concern. *J Vasc Surg.* 2014; 60:865–873.
- Donas KP, Torsello GB, Piccoli G, et al. The PROTAGORAS study to evaluate the performance of the Endurant stent graft for patients with pararenal pathologic processes treated by the chimney/snorkel endovascular technique. *J Vasc Surg.* 2016;63:1–7.
- Iezzi R, Di Stasi C, Dattesi R, et al. Proximal aneurysmal neck: angiography conformational pulsatile changes with possible consequences for endograft sizing. *Radiology.* 2011;260:591–598.
- van Keulen JW, Moll FL, Barwegen GK, et al. Pulsatile distension of the proximal aneurysm neck is larger in patients with stent graft migration. *Eur J Vasc Endovasc Surg.* 2010;40:326–331.
- de Bruin JL, Yeung KK, Niepoth WW, et al. Geometric study of various chimney graft configurations in an in vitro juxtarenal aneurysm model. *J Endovasc Ther.* 2013;20:184–189.
- Parodi JC, Berguer R, Ferreira LM, et al. Intra-aneurysmal pressure after incomplete endovascular exclusion. *J Vasc Surg.* 2001;34:909–914.
- Lehmkuhl L, Andres C, Lücke C, et al. Dynamic CT angiography after abdominal aortic endovascular aneurysm repair: influence of enhancement patterns and optimal bolus timing on endoleak detection. *Radiology.* 2013;268:1–7.
- Iezzi R, Cotroneo AR, Filippone A, et al. Multidetector-row computed tomography angiography in abdominal aortic aneurysm treated with endovascular repair: evaluation of optimal timing of delayed phase imaging for the detection of low-flow endoleaks. *J Comput Assist Tomogr.* 2008;32:609–615.
- Groot Jebbink E, Mathai V, Boersen JT, et al. Hemodynamic comparison of stent configurations used for aortoiliac occlusive disease. *J Vasc Surg.* 2017;66:251.e1–260.e1.
- Yousif MY, Holdsworth DW, Poepping TL. A blood-mimicking fluid for particle image velocimetry with silicone vascular models. *Exp Fluids.* 2011;50:769–774.
- Lanne T, Bergqvist D, Bengtsson H, et al. Diameter and compliance in the male human abdominal aorta: influence of age and aortic aneurysm. *Eur J Vasc Surg.* 1992;6:178–184.
- van Herwaarden JA, Bartels LW, Muhs BE, et al. Dynamic magnetic resonance angiography of the aneurysm neck: conformational changes during the cardiac cycle with possible consequences for endograft sizing and future design. *J Vasc Surg.* 2006;44:22–28.
- Patel RP, Katsargyris A, Verhoeven EL, et al. Endovascular aortic aneurysm repair with chimney and snorkel grafts: indications, techniques and results. *Cardiovasc Intervent Radiol.* 2013;36:1443–1451.
- Bosiers MJ, Donas KP, Mangialardi N, et al. European multicenter registry for the performance of the chimney/snorkel technique in the treatment of aortic arch pathologic conditions. *Ann Thorac Surg.* 2016;101:2224–2230.
- Ullery BW, Itoga NK, Tran K, et al. Natural history of type Ia gutter endoleaks after snorkel/chimney EVAR. *J Vasc Surg.* 2017;65:981–990.
- Moll FL, Powell JT, Fraedrich G, et al. Management of abdominal aortic aneurysms clinical practice guidelines of the European Society for Vascular Surgery. *Eur J Vasc Endovasc Surg.* 2011;41(suppl 1):S1–S58.
- Bastos Gonçalves F, Verhagen HJ, Vasanthanathan K, et al. Spontaneous delayed sealing in selected patients with a primary type-Ia endoleak after endovascular aneurysm repair. *Eur J Vasc Endovasc Surg.* 2014;48:53–59.
- Lachat M, Veith FJ, Pfammatter T, et al. Chimney and periscope grafts observed over 2 years after their use to revascularize 169 renovisceral branches in 77 patients with complex aortic aneurysms. *J Endovasc Ther.* 2013;20:597–605.
- Mestres G, Uribe JP, García-Madrid C, et al. The best conditions for parallel stenting during EVAR: an in vitro study. *Eur J Vasc Endovasc Surg.* 2012;44:468–473.
- Tessarek J. BeGraft peripheral stent design and technical aspects. Paper presented at: LINC Congress 2016; January 27, 2016; Leipzig, Germany. https://linc2016.cncptdlx.com/media/1235_Joerg_Tessarek_27_01_2016_Room_5_Global_Expert_Exchange.pdf. Accessed February 6, 2018.